The EMBO Journal (2012) 31, 3252–3269 | © 2012 European Molecular Biology Organization | Some Rights Reserved 0261-4189/12
www.embojournal.org

THE EMBO JOURNAL

EMBO open

ARF6-mediated endosomal transport of Telencephalin affects dendritic filopodia-to-spine maturation

Tim Raemaekers[1,3,*], Aleksandar Peric[1,3], Pieter Baatsen[2], Ragna Sannerud[1], Ilse Declerck[1], Veerle Baert[1], Christine Michiels[1] and Wim Annaert[1,*]

[1]Laboratory of Membrane Trafficking, Center for Human Genetics, KU Leuven and VIB Center for the Biology of Disease, Leuven, Belgium and [2]Electron Microscopy Facility (EMCORF), VIB Center for the Biology of Disease, Leuven, Belgium

Dendritic filopodia are dynamic structures thought to be the precursors of spines during synapse development. Morphological maturation to spines is associated with the stabilization and strengthening of synapses, and can be altered in various neurological disorders. Telencephalin (TLN/intercellular adhesion molecule-5 (ICAM5)) localizes to dendritic filopodia, where it facilitates their formation/maintenance, thereby slowing spine morphogenesis. As spines are largely devoid of TLN, its exclusion from the filopodia surface appears to be required in this maturation process. Using HeLa cells and primary hippocampal neurons, we demonstrate that surface removal of TLN involves internalization events mediated by the small GTPase ADP-ribosylation factor 6 (ARF6), and its activator EFA6A. This endocytosis of TLN affects filopodia-to-spine transition, and requires Rac1-mediated dephosphorylation/release of actin-binding ERM proteins from TLN. At the somato-dendritic surface, TLN and EFA6A are confined to distinct, flotillin-positive membrane subdomains. The co-distribution of TLN with this lipid raft marker also persists during its endosomal targeting to CD63-positive late endosomes. This suggests a specific microenvironment facilitating ARF6-mediated mobilization of TLN that contributes to promotion of dendritic spine development.

The EMBO Journal (2012) **31,** 3252–3269. doi:10.1038/emboj.2012.182; Published online 10 July 2012
Subject Categories: membranes & transport; neuroscience
Keywords: ARF6; EFA6A; flotillin; spine morphogenesis; Telencephalin

Introduction

Dendritic filopodia are long, thin, actin-rich, and dynamic protrusions that are considered to be the precursors of mature, mushroom-shaped spines, both during early neural development and later into adulthood (Yuste and Bonhoeffer, 2004). This maturation process that generates post-synaptic sites of synapses is reversible, and reflects the plastic nature of synaptic connections (Matus, 2000). Alterations of the underlying remodelling machinery can result in abnormal spine structures, as seen in various neurological disorders including Fragile X syndrome and Alzheimer's disease (AD) (Kaufmann and Moser, 2000; Knafo *et al*, 2009). Since the mechanism driving spine morphogenesis is still unclear, gaining further insight herein remains an important challenge.

Telencephalin (TLN), also known as intercellular adhesion molecule-5 (ICAM5), plays an important role in spine morphogenesis. It prominently localizes to dendritic filopodia where it facilitates their formation and maintenance in a process that requires actin-binding ERM (ezrin/radixin/moesin) proteins (Matsuno *et al*, 2006; Furutani *et al*, 2007). In contrast to other adhesion molecules, TLN slows maturation and stabilization of synapses. In agreement, TLN deficiency or knockdown of ERM proteins increases spine maturation, while overexpression of TLN or constitutively active ezrin favours more filopodia (Matsuno *et al*, 2006; Furutani *et al*, 2007). Although the exact mechanism governing filopodia to spine transition is still unclear, it may require exclusion of TLN from filopodia, as spines are largely devoid of it (Yoshihara *et al*, 2009). We hypothesize that this is most likely mediated by until now unexplored internalization events, aside of the already described proteolytic shedding of TLN (Tian *et al*, 2007).

We previously demonstrated that TLN accumulates aberrantly and prominently in presenilin1 (PSEN1)-deficient hippocampal neurons, as opposed to culture-matched wild-type neurons (Annaert *et al*, 2001; Esselens *et al*, 2004). PSEN1 is a key component of the γ-secretase complex important in AD (De Strooper and Annaert, 2010). It interacts with TLN, but rather than cleaving it, PSEN1 modulates its trafficking in a γ-secretase-independent manner (Esselens *et al*, 2004). Importantly, intracellular entrapment of TLN may affect its normal surface levels/function. As aberrant endosomal trafficking and synaptic dysfunctions have both been described as early stage events in various neurodegenerative diseases, including AD (Pimplikar *et al*, 2010), we searched for regulators of internalization/trafficking of TLN, and explored how they affect its role in spine morphogenesis.

The small GTPase, ADP-ribosylation factor 6 (ARF6), is known to regulate endosomal trafficking and actin dynamics (D'Souza-Schorey and Chavrier, 2006; Grant and Donaldson, 2009). Its role herein has been mostly studied in HeLa cells, while in neurons, ARF6 was shown to participate in spine morphogenesis, where its activation by the guanine nucleotide exchange factor (GEF), EFA6A (Sakagami, 2008), promoted formation and maintenance of spines in a Rac1-dependent manner (Choi *et al*, 2006). This clearly contrasts

*Corresponding authors. T Raemaekers or W Annaert, Laboratory of Membrane Trafficking, Center for Human Genetics, KU Leuven and VIB Center for the Biology of Disease, Campus Gasthuisberg, POB 602, O&N4, Room 7.159, Leuven, Belgium. Tel.: +32 16 330520; Fax: +32 16 330939; E-mail: wim.annaert@cme.vib-kuleuven.be or tim.raemaekers@gbiomed.kuleuven.be
[3]These authors contributed equally to this work

Received: 6 September 2011; accepted: 11 June 2012; published online: 10 July 2012

the aforementioned function of TLN in slowing spine maturation (Matsuno *et al*, 2006). In this study, we demonstrate that (i) TLN recruits EFA6A and (ii) requires ARF6-activation for internalization. We furthermore show that its endosomal targeting to CD63-positive multivesicular bodies (MVBs)/late endosomes involves the association with flotillin-positive microdomains.

Collectively, our data support the ARF6-dependent mobilization of TLN from dendritic filopodia, which consequently contributes to their maturation into spines.

Results

TLN and the ARF6 activator, EFA6A, interact in vitro, and associate with flotillin-positive domains in neurons

In order to identify novel regulators of TLN internalization, we focused on proteins involved in membrane trafficking and spine development. We opted to assess if the endogenous distribution pattern of such candidates changed as a consequence of an induced change in the somato-dendritic localization of TLN. We established previously that the addition of polystyrene microbeads to primary hippocampal neurons results in a marked re-distribution of TLN to the microbead attachment sites (Esselens *et al*, 2004). TLN appears to act here specifically as microbeads seem not to adhere to axons (Supplementary Figure S1), nor to young neurons (Supplementary Figure S2), both of which are devoid of TLN. The feature of TLN herein is further reinforced by the lack of prominent recruitment to such sites of another dendritic cell adhesion protein, N-Cadherin (Figure 1A).

Interestingly, we showed that the cup-like dendritic protrusions at microbead attachment sites also contain phosphatidylinositol 4,5-biphosphate (PIP2; Esselens *et al*, 2004). PIP2 is a surface-associated phospholipid generated by phosphatidylinositol 4-phosphate 5-kinase (PIP5-kinase) upon its activation by ARF6 (Brown *et al*, 2001). Besides regulating endosomal transport and actin dynamics (D'Souza-Schorey and Chavrier, 2006), ARF6 also promotes spine development (Choi *et al*, 2006), making it a prime candidate regulator of TLN trafficking. As the ARF6-GEF, EFA6A, has a similar somato-dendritic localization (Sakagami *et al*, 2007; Sannerud *et al*, 2011) as TLN, we first tested if it co-enriched with TLN at microbead attachment sites in hippocampal neurons and (transfected) HeLa cells. HeLa cells do not normally express TLN, but they do offer the advantage of working with a well-established cell system for studying EFA6A/ARF6-related trafficking (Donaldson *et al*, 2009). For transfection experiments in HeLa cells and in neurons, we tagged TLN with an internal, transmembrane proximal mCherry/mRFP tag (Figure 4A), thereby keeping both protein termini free for physiologically relevant interactions (Tian *et al*, 2000; Furutani *et al*, 2007). This internal tag did not interfere with TLN's recruitment and attachment to microbeads (Figure 1A; Supplementary Figure S3), nor does it affect its somato-dendritic polarization during development (Nicolaï *et al*, 2010). In both differentiated hippocampal neurons and co-transfected HeLa cells, EFA6A was indeed co-recruited with TLN to microbeads (Figure 1A).

Next, we analysed the distribution of endogenous EFA6A/ARF6 and TLN in 14 DIV hippocampal neurons and showed that as expected they have closely overlapping distribution along the dendritic shaft and within filopodia. At the basal surface of neuronal cell bodies, they also displayed a strikingly similar mesh-like pattern (Figure 1B and D), suggesting their mutual preference for a defined membrane (lipid/protein) microenvironment. This is further strengthened by the observation that N-Cadherin has a more homogeneous surface distribution (Supplementary Figure S4). Interestingly, the nature of these microdomains is distinct from that of focal adhesion molecules as both vimentin and α-actinin are excluded from TLN-positive domains in TLN-expressing HeLa cells, where a reminiscent surface distribution of TLN is observed (Supplementary Figure S4). On the other hand, the lipid raft-associated protein flotillin/reggie displays a similar distribution (Neumann-Giesen *et al*, 2004) and our co-expression analysis of tagged TLN and flotillin2 in HeLa cells (Supplementary Figure S5) and in hippocampal neurons (Figure 1C and D) also confirms this. Here, along dendrites, both proteins were closely apposed within filopodia and in the shaft (Figure 1C), where the patchy staining pattern often persisted. This congruent microdomain association of expressed TLN and flotillin is further supported through their mutual recruitment to microbeads added to HeLa cells (Supplementary Figure S6) and the ability to, unlike N-Cadherin, resist the detergent extraction in neurons (Supplementary Figure S7; Ledesma *et al*, 1998).

As EFA6A co-distributes with TLN we next assessed their interaction biochemically. EFA6A was previously shown to interact with two neuronal potassium channels, both depending on ARF6 for their trafficking (Decressac *et al*, 2004; Gong *et al*, 2007). Using similar co-immunoprecipitation conditions, we show in a reciprocal set-up (Figure 1E; Supplementary Figure S8) that EFA6A may indeed interact (in)directly with TLN and that this interaction could depend on the presence of the intracellular domain of TLN.

Taken together, these data suggest that TLN and EFA6A may associate with flotillin-positive membrane domains. The relevance of these observations is underscored by the fact that flotillin, like EFA6A, plays a role in protein trafficking (Stuermer, 2010), has synaptic functions (Swanwick *et al*, 2010b), and as TLN, affects filopodia formation (Neumann-Giesen *et al*, 2004).

Trafficking of TLN is regulated by ARF6 and its internalization involves EFA6A-mediated activation of ARF6

ARF6 regulates the trafficking of specific plasma-membrane proteins by switching from a GDP- to an active GTP-bound form via an exchange activity mediated by EFA6A (Figure 2C; D'Souza-Schorey and Chavrier, 2006; Franco *et al*, 1999). As TLN can interact with EFA6A, we therefore studied how altering the activation state of ARF6 affects the localization of TLN. When expressed alone in HeLa cells, TLN is found almost exclusively at the cell surface, localizing to filopodia and microvilli-like structures, which are induced by its expression (Figure 2A). On the contrary, co-expression with EFA6A causes filopodia and microvilli-like structures to disappear and TLN to redistribute from the surface to a punctate vesicular localization. This likely reflects its enhanced internalization, as these punctae are not immunostained by a TLN ectodomain-specific antibody in non-permeabilized cells (Figure 2A and B; Supplementary Figure S9, and see later). This agrees with the role of EFA6A in co-ordinating endo-

cytosis with cytoskeletal remodelling at the cell surface, both requiring the activity of ARF6 and its downstream target, the Rho family GTPase, Rac1 (Franco *et al*, 1999; Figure 2C). To demonstrate that EFA6A-mediated TLN internalization indeed occurs via ARF6 activation, we co-expressed TLN/EFA6A with ARF6T27N, a dominant mutant keeping ARF6 in its GDP-locked state. As expected, here we noticed little or no TLN internalization, while

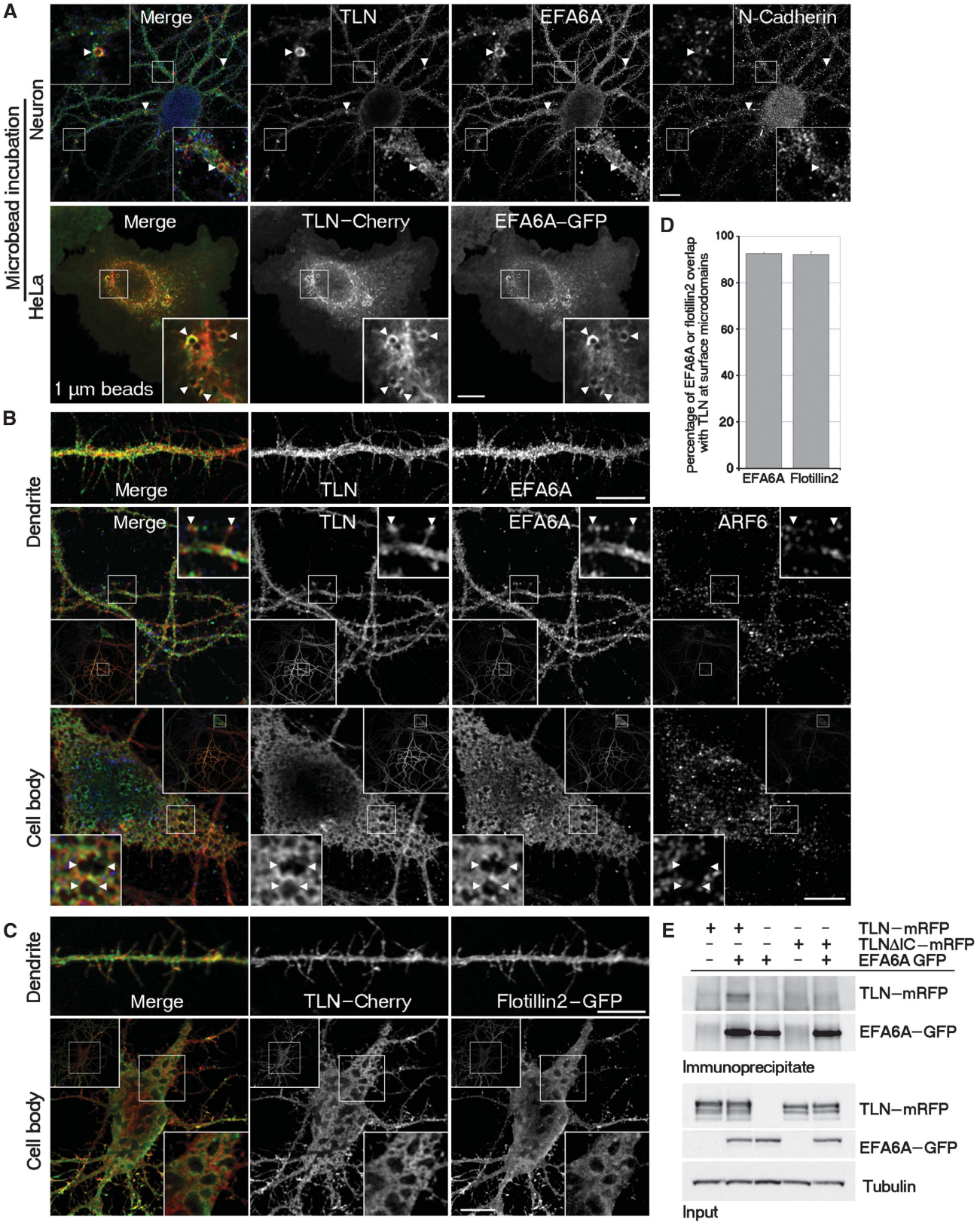

filopodia and microvilli-like structures remained preserved (Figure 2A and B).

We next studied how ARF6 activation affects intracellular sorting of TLN using well-described ARF6 mutants, including ARF6T27N and the GTP-locked (constitutively active) ARF6Q67L. In HeLa cells, expression of ARF6Q67L results in the accumulation of grape-like vacuoles in which ARF6-cargo proteins like MHCI and CD59 are trapped (Naslavsky *et al*, 2004). Likewise, co-expressed TLN readily colocalized with MHCI in ARF6Q67L-positive endosomal structures (Figure 2D). ARF6 cargos, like MHCI and CD59, internalize in a clathrin-independent manner as opposed to, e.g., the transferrin receptor (TfR) that uses clathrin-mediated endocytosis (Naslavsky *et al*, 2004). As such, TfR, did not accumulate in ARF6Q67L vacuoles, thereby underscoring the selective ARF6-dependent endosomal sorting of TLN (Supplementary Figure S10). Importantly, in primary hippocampal neurons, endogenous as well as overexpressed TLN similarly accumulated in ARF6Q67L vacuoles (Figure 2D). On the other hand, the GDP-locked mutant ARF6T27N is known to block recycling of specific ARF6 cargos from a perinuclear recycling compartment to the cell surface (D'Souza-Schorey *et al*, 1998; Sannerud *et al*, 2011). Expectedly, upon co-expression with ARF6T27N in HeLa cells, TLN co-accumulated with ARF6T27N and endogenous CD59 in discrete perinuclear compartments (Supplementary Figure S11). Notably, colocalization of expressed TLN and ARF6T27N was also observed in hippocampal neurons (Supplementary Figure S12).

Taken together, these data identify TLN as a novel cargo protein of ARF6-mediated internalization and endosomal sorting.

Internalization of TLN involves Rac1-mediated actin remodelling, ERM dephosphorylation as well as its release from binding to ERM proteins

As Rac1 activity is required for ARF6-mediated spine maturation (Choi *et al*, 2006), we tested how this downstream target of ARF6 (Figure 3D; Franco *et al*, 1999; Koo *et al*, 2007) affects TLN localization. In HeLa cells, co-expression of TLN with a dominant active Rac1 mutant (GTP-bound Rac1V12; Ridley *et al*, 1992) resulted in prominent dorsal ruffling and endocytosis of TLN (Figure 3A). Cortical actin polymerization/remodelling underlies membrane ruffling (Franco *et al*, 1999) and is usually accompanied by the uptake of large portions of extracellular fluid (macropinocytosis) (Donaldson *et al*, 2009). To assess if internalized TLN indeed arises from macropinocytic uptake, we incubated TLN/Rac1V12-expressing cells with 70 kDa dextran beads. Confocal analysis indeed revealed a clear colocalization of a part of TLN-positive endosomes with this macropinocytic marker (Figure 3B).

As interaction of TLN with phosphorylated ERM (pERM) proteins is essential for its surface anchorage and function in filopodia formation/maintenance (Furutani *et al*, 2007), we next show that in addition to TLN internalization, Rac1 activation also causes a general reduction in staining intensity of pERMs (Figure 3C). This implies that the mechanism of TLN endocytosis could involve ERM dephosphorylation. Earlier studies in lymphocytes reported that Rac1-mediated dephosphorylation of ERMs translated into disassembly of microvilli via a loss of anchorage of membrane proteins to the underlying actin cytoskeleton (Faure *et al*, 2004; Nijhara *et al*, 2004; Figure 3D). Thus, we tested whether disrupting the TLN–ERM interaction is sufficient to induce TLN internalization (Figure 3E). Co-expression of TLN with the FERM domain of ERM proteins (which binds the cytosolic domain of target proteins including TLN, but not actin; Amieva *et al*, 1999; Allenspach *et al*, 2001), outcompeted binding of endogenous pERMs to TLN, resulting in the emergence of TLN-positive endosomal punctae, both in HeLa cells and in neurons (Figure 3E). Together, these data demonstrate the dependence of TLN internalization on Rac1-mediated cortical actin remodelling and ERM dephosphorylation.

Deletion of an acidic cluster/ERM-binding domain of TLN enhances its internalization

To elucidate further the endosomal route of TLN, we searched for sorting motifs within its cytosolic domain (Figure 4A). As sequence homology searches did not conclusively reveal any known sorting sequences, and in light of our findings (Figure 3), we hypothesized that the deletion of the ERM-binding domain of TLN on its own may be sufficient to facilitate its internalization. Previously, it has been suggested that ERM binding to TLN requires well-conserved amino-acid residues (Furutani *et al*, 2007), which we now show are situated within a conserved acidic cluster (AC) (Figure 4A), slightly resembling the EX motif of the KAC (potassium channel AC), a sorting sequence involved in ARF6-mediated trafficking (Gong et al, 2007). We therefore generated a mutant TLN in which the AC was deleted (TLNΔAC).

Expression of TLNΔAC in HeLa cells resulted in a loss of staining for active pERM proteins and fewer filopodia/microvilli-like stuctures, as compared to full-length TLN. This was

Figure 1 Telencephalin and EFA6A interact *in vitro*, and associate with flotillin-positive domains in neurons. (**A**) Top panel: Hippocampal neurons (DIV 14) were incubated overnight with polystyrene microbeads (1 μm) and stained for TLN (red), EFA6A (green) and N-Cadherin (blue). Arrowheads indicate microbead attachment sites, where TLN and EFA6A, but not N-Cadherin are strongly co-enriched. Bottom panel: as in the top panel but using HeLa cells co-expressing TLN–Cherry and EFA6A–GFP. (**B**) Hippocampal neurons (DIV 14) were stained for endogenous TLN (red) and EFA6A (green) with or without ARF6 (blue). Top panel: Dendrite showing the close association of TLN and EFA6A. Note that each TLN-positive filopodium also contains EFA6A. Middle and bottom panels: TLN and EFA6A are closely apposed to ARF6 within filopodia as well as at the cell body, where the staining pattern of the three proteins appears confined to distinct surface microdomains (arrowheads). (**C**) Hippocampal neurons (DIV 14) co-expressing TLN–Cherry and flotillin2–GFP. Both proteins show, as in (**B**), a similar distribution along dendrites and at the cell body. (**D**) Acquired images (see **B**, **C**) were analysed for overlap between TLN and EFA6A or flotillin2 at the surface microdomains. Data were collected and averaged from several independent neurons and depicted in graphs. The obtained percentages are for EFA6A: 92.5 ± 0.4, and flotillin2: 92.1 ± 1.2. (**E**) Cell lysates obtained from HeLa cells co-expressing either TLN–mRFP or a cytosolic-domain deletion mutant of TLN (ΔIC) and/or EFA6A–GFP, as indicated on the top, were subjected to co-immunoprecipitation experiments with anti-GFP Ab. Note that in contrast to full-length TLN, TLNΔIC did not co-immunoprecipitate with EFA6A. Bars: 10 μm.

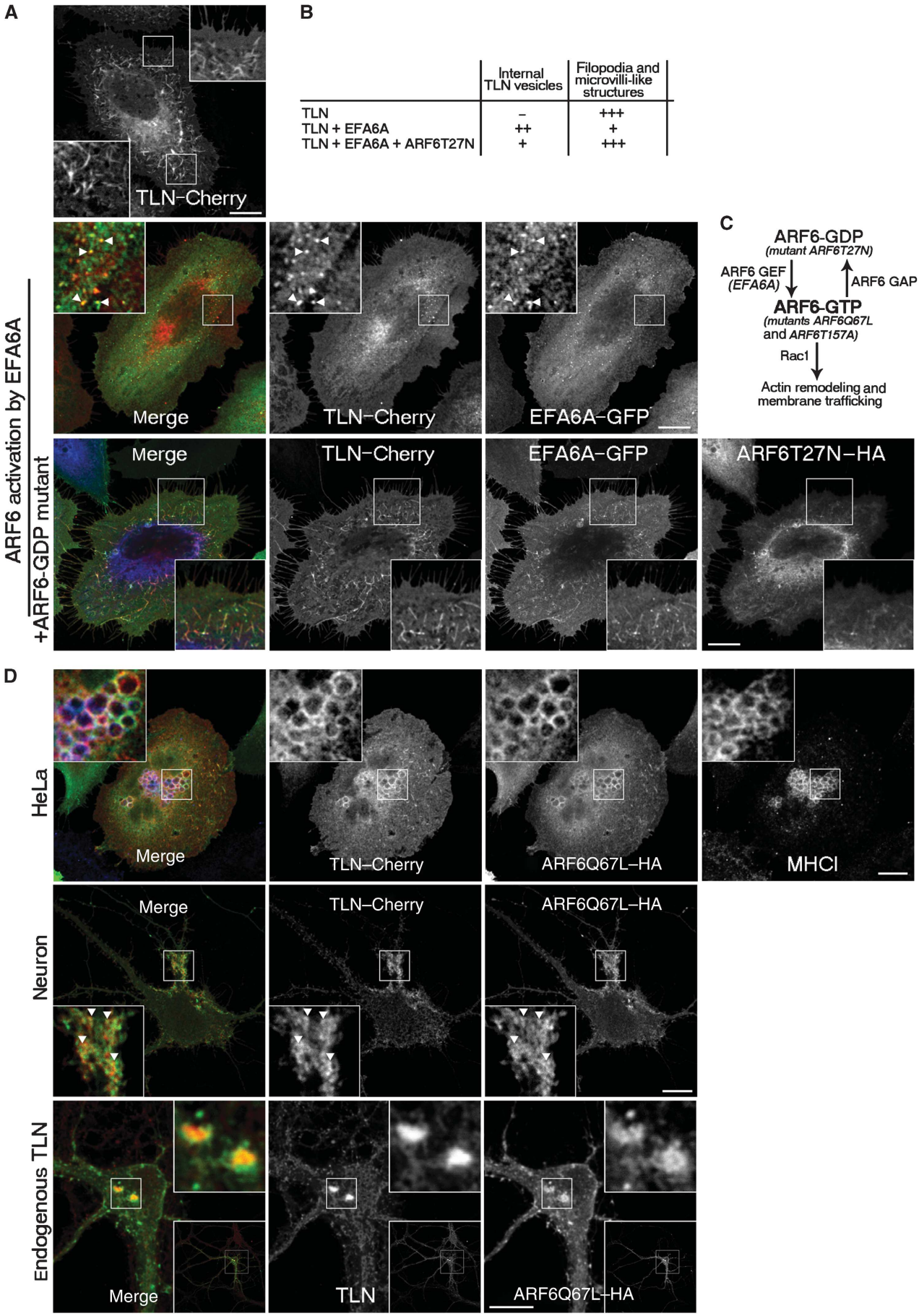

paralleled by a clear redistribution of TLNΔAC towards a more internal localization (Figure 4B). Moreover, the observation that TLNΔAC still got trapped in the ARF6Q67L compartment (Supplementary Figure S13) suggests that the AC of TLN does not affect its ARF6-dependent routing, but rather plays a role in its surface retention, likely by binding the ERM proteins.

To quantify the differential internalization of TLNΔAC relative to full-length TLN, we co-expressed each construct together with the dominant active GTP-locked RAB5 mutant (RAB5Q79L; Stenmark *et al*, 1994). This mutant blocks sorting and recycling from early endosomes resulting in the accumulation of surface-internalized cargos in enlarged RAB5 endosomes. This approach allowed us to clearly discriminate between surface-associated and endosomal TLN. As expected, in both HeLa cells and primary neurons, TLNΔAC accumulated more prominently in RAB5Q79L-positive enlarged endosomes compared to full-length TLN (Figure 4C and D). Using an antibody uptake assay, we could furthermore demonstrate that TLNΔAC in Rab5Q79L-containing endosomes indeed originates from the cell surface (Supplementary Figure S14). Noteworthy, these experiments additionally showed that TLN has very slow internalization kinetics, as a 2-h uptake after surface labelling was required for its detection in Rab5Q79L endosomes. Such slower kinetics is reminiscent to that of other ARF6-cargo proteins, like for instance BACE1 (Sannerud *et al*, 2011).

Collectively, these findings demonstrate that TLNΔAC, a deletion mutant with disrupted ERM-binding capacity, has a more prominent surface to endosomal routing as compared to full-length TLN. This is in agreement with the relative exclusion of TLN from mature spines (Matsuno *et al*, 2006), where the functional interaction between pERM and TLN does not take place (Furutani *et al*, 2007). Moreover as knockdown of ERM proteins promotes spine maturation, while expression of a constitutively active ERM (ezrin) mutant results in more dendritic filopodia (Furutani *et al*, 2007), our data extend these reports by providing a missing link between TLN–ERM interaction, TLN internalization and filopodia-to-spine maturation.

ARF6-mediated TLN internalization contributes to filopodia-to-spine maturation

Activation of ARF6, by either expression of EFA6A or the ARF6 fast-cycling mutant (ARF6T157A; Santy, 2002), promotes spine formation and reduces filopodia number (Choi *et al*, 2006). However, expression of TLN is known to cause the opposite effect (Matsuno *et al*, 2006). We therefore postulated that ARF6-driven internalization of TLN from the cell surface may constitute a contributing factor that promotes spine development.

To test this, we compared the effects of ARF6 activation on spine development in culture-matched wild-type and TLN knockout ($TLN^{-/-}$) primary hippocampal neurons (Supplementary Figure S15). We used the same experimental conditions as in Choi *et al* (2006) and expressed in both neuronal genotypes the fast-cycling mutant (ARF6T157A; active), the dominant-negative mutant (ARF6T27N; inactive), or farnesylated GFP (fGFP) alone as a control. In wild-type ($TLN^{+/+}$) neurons, ARF6T157A expression induced a significant decrease in the number of filopodia (and concomitant increase in spine number) when compared to fGFP alone (Figure 5A and B). This effect was not observed for the ARF6 inactive mutant ARF6T27N. Interestingly, in TLN-deficient neurons, the promoting effect of ARF6T157A in filopodia-to-spine transition was reduced almost by half (from 8.7% relative difference in wild type to only 4.7% relative difference in $TLN^{-/-}$ neurons). Like in $TLN^{+/+}$ neurons, expression of inactive ARF6T27N here as well did not affect spine density. These findings imply a partial yet significant (negative) contributing role of TLN in ARF6-driven spine maturation and suggest that ARF6-mediated mobilization of TLN from the filopodial surface may indeed contribute to and in part explain the promoting effect of ARF6 activation herein. However, this complex process of spine morphogenesis, in which ARF6 participates in, likely requires a well-orchestrated balance of contributions from several other key molecules as well.

To determine whether this partial contribution to spine maturation of TLN is mediated via its ARF6 activity-dependent removal/internalization from the cell surface (filopodia), like we observed in HeLa cells (Figure 6A), and in line with our previous findings (Figures 2–4), we next stained neurons for: (1) fGFP to define the membrane periphery, (2) synaptophysin to control for synapse density, and (3) TLN to determine its relative distribution along dendrites (surface versus internal). A quantitiative analysis showed that in neurons expressing ARF6T157A, endogenous TLN co-distributes less with surface-anchored fGFP, as compared to those expressing ARF6T27N (Figure 6B). This implies that ARF6 activation results in a more central localization of TLN within the dendritic shaft, suggesting an increased internalization. Because the kinetics of endogenous TLN internalization is very slow (see above, Supplementary Figure S14) and in order to further discriminate between internal and surface localized TLN in primary neurons, we

Figure 2 Trafficking of Telencephalin is regulated by ARF6 and its internalization involves EFA6A-mediated activation of ARF6. (**A**) Top panel: HeLa cell expressing TLN–Cherry. Insets highlight the presence of TLN at filopodia and microvilli-like structures evident at the apical surface. Middle panel: HeLa cells co-expressing TLN–Cherry and EFA6A–GFP. Arrowheads indicate internal vesicles containing both TLN and EFA6A. Lower panel: as in the middle panel, but co-expressed with ARF6T27N–HA (inactive ARF6), and stained for HA (blue). Note that TLN is hardly internalized and filopodia and microvilli-like structures remain intact. (**B**) List summarizing the presence/abundance of intracellular TLN-containing vesicles and filopodia/microvilli-like structures, when TLN is expressed alone, or in combination with EFA6A with or without ARF6T27N. More than 100 randomly selected cells from three independent experiments were analysed. (**C**) Literature-based scheme that depicts how inactive GDP-bound ARF6 gets activated to GTP-bound ARF6 by its GEF, EFA6A. The mutants used in the study (ARF6Q67L, ARF6T157A, ARF6T27N), and the activation state which they reflect, are also indicated. Note that ARF6-induced actin remodelling and membrane trafficking is dependent on Rac1. (**D**) Top panel: HeLa cells co-expressing TLN–Cherry and ARF6Q67L–HA were stained for HA (green) and the ARF6-cargo protein, MHCI (blue). All three proteins are clearly entrapped within the grape-like vacuoles. Middle panel: Hippocampal neurons (DIV 14) co-expressing TLN–Cherry and ARF6Q67L–HA. Arrowheads indicate TLN entrapment in vacuole-like structures that resemble those observed in HeLa cells. Bottom panel: Hippocampal neurons (DIV 14) expressing the ARF6Q67L–HA were stained for endogenous TLN (red) and HA (green). Note the clear entrapment of TLN in ARF6Q67L vacuoles. Bars: 10 μm.

co-expressed TLN and RAB5Q79L with the respective ARF6 mutants. This demonstrated that the fast-cycling ARF6T157A, but not the inactive ARF6T27N indeed caused a more marked entrapment of TLN in somato-dendritically localized RAB5Q79L-positive enlarged endosomes, thereby confirming a more pronounced endocytosis of TLN when ARF6 is activated.

We next assessed the effect of ARF6 knockdown on TLN distribution by using lentiviral particles expressing shRNAs targeting ARF6. Levels of ARF6 were knocked down to 30% relative to the control (Supplementary Figure S16), and this resulted in an increase in both TLN levels and the total/average length of TLN-positive dendritic protrusions. These results indicate a more abundant surface (functional) locali-

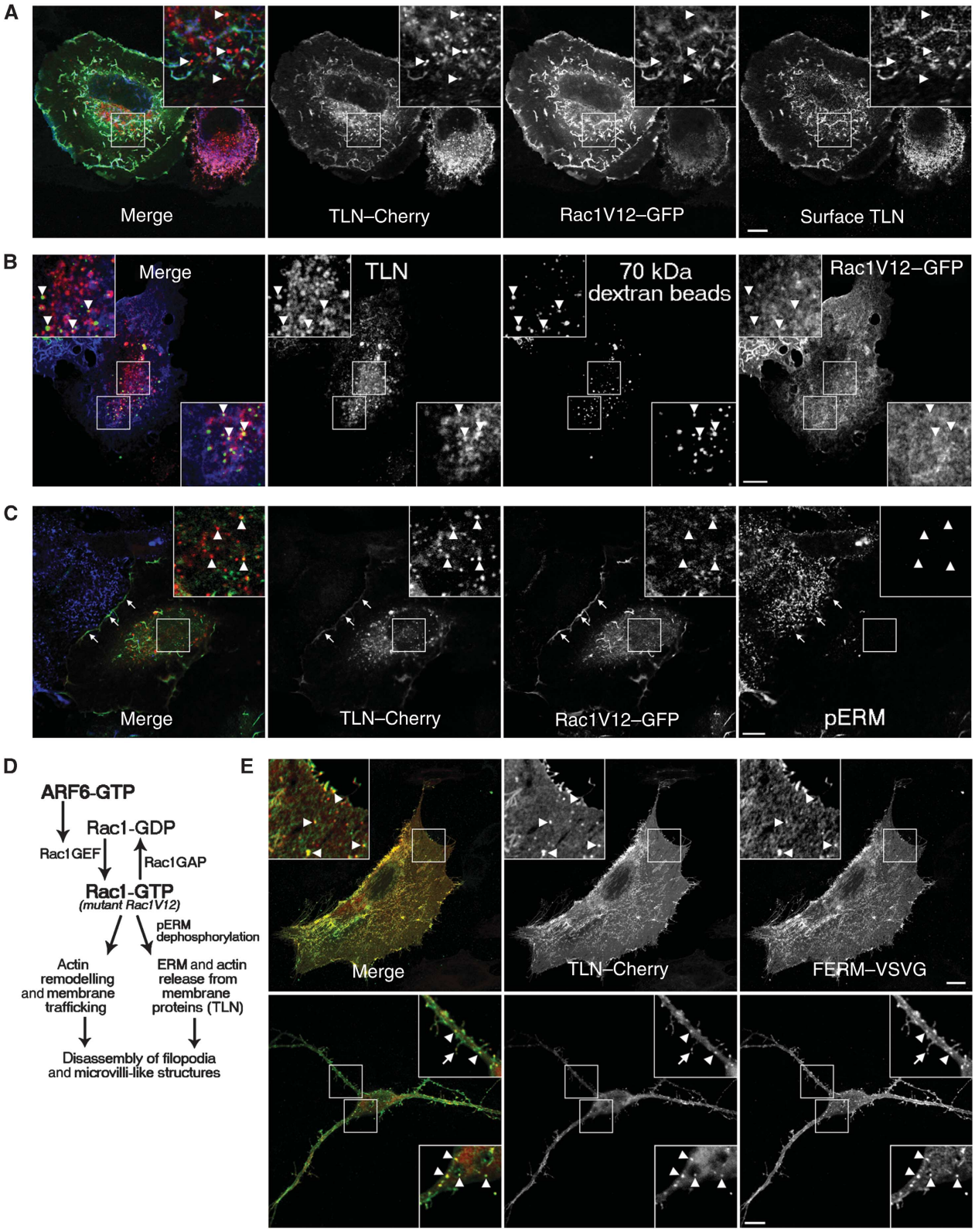

zation of TLN, that not only agrees with a role of ARF6 in internalization and endosomal transport of TLN, but is also in line with an earlier report describing the stimulatory effect of TLN expression on filopodia formation (Matsuno *et al*, 2006).

Collectively, these findings provide novel insights into the molecular mechanism of ARF6-mediated promotion of spine morphogenesis, by demonstrating its involvement in the removal of TLN from dendritic filopodia.

Internalized TLN is routed to CD63-positive MVBs

To further elucidate the endosomal itinerary of TLN, which could also affect its surface presence/function, we expressed TLNΔAC in HeLa cells and observed it colocalizing with CD63 (Figure 7A), a marker of late endosomes/MVBs (Pols and Klumperman, 2009). An antibody uptake assay further shows that TLNΔAC in CD63-positive endosomes originates from the cell surface (Figure 7B), while immuno-electron microscopy (EM) clearly demonstrates its localization within intralumenal vesicles (ILVs) of MVBs (Figure 7C). This implies that following internalization TLN is routed to lysosomal degradation and/or exosomal release. Interestingly, RAB5Q79L-induced enlarged endosomes were also recently shown to acquire certain MVB features, including formation of ILVs, thereby resembling CD63-containing late endosomes (Wegner *et al*, 2010). In agreement, co-expression of TLNΔAC with RAB5Q79L indeed resulted in their marked colocalization with CD63 (Supplementary Figure S17). Herein, TLNΔAC and CD63 colocalized on ILVs, as demonstrated by subsequent immuno-EM analysis (Supplementary Figure S17). Finally in hippocampal neurons the tagged TLNΔAC and CD63 were also found colocalizing in the cell body and along the dendritic shaft (Figure 7D), thereby underscoring that also in neurons, following internalization, TLN can be targeted to CD63-positive MVBs.

As flotillin is known to be concentrated in ILVs of MVBs and exosomes (de Gassart *et al*, 2003) and since we showed that TLN and flotillin co-distribute in similar mesh-like membrane subdomains (Figure 1C and D), this prompted us to look in more detail into the endosomal localization of TLN and flotillin. In HeLa cells co-expressing tagged TLNΔAC and flotillin2/flotillin1 almost 70% of flotillin-positive endosomes indeed contain TLNΔAC (Figure 8A; Supplementary Figure S18). This was also confirmed in hippocampal neurons where tagged TLN and flotillin2/flotillin1 co-distributed internally in the cell body and along the dendrites, where numerous vesicles were found containing both proteins (Figure 8B; Supplementary Figure S18).

Finally, we previously demonstrated that in PSEN1-deficient hippocampal neurons, and to a lesser degree in culture-matched wild-type neurons, TLN accumulates aberrantly in distinct intracellular vacuoles that do not co-stain for a number of intracellular marker proteins of the biosynthetic and endosomal pathways (Annaert *et al*, 2001; Esselens *et al*, 2004). We now show that in mature wild-type neurons (DIV 26), both endogenous CD63 and the flotillin2 can co-accumulate with TLN in these vacuoles (Figure 8C). This further strengthens our findings by implying that these proteins are mutually associated with a related trafficking route, which under certain (stress) conditions, can potentially get altered.

Discussion

Despite TLN's important role as a negative regulator of spine development, both its internalization and trafficking, which likely affects its surface function, have hardly been explored. One of the factors that regulates trafficking of surface proteins, and also mediates spine maturation is ARF6 (Choi *et al*, 2006; D'Souza-Schorey and Chavrier, 2006). Because its role contrasts that of TLN (Matsuno *et al*, 2006), we hypothesized that ARF6 is involved in the internalization and trafficking of TLN. Our findings show that: (1) TLN internalization is indeed regulated by ARF6 and involves its activation by EFA6A; (2) in neurons this partially contributes to ARF6-mediated promotion of spine development; (3) the underlying mechanism requires Rac1-mediated actin remodelling and release of ERM-binding to TLN, while (4) further trafficking of TLN involves the lipid raft marker flotillin, and targeting to the CD63-containing late endosomal/MVBs.

These findings allow us to propose a model for the regulated trafficking of TLN in hippocampal neurons (Figure 9). By binding EFA6A, TLN confines its activity within the dendritic filopodium. Herein, EFA6A activates ARF6, which subsequently triggers Rac1 activity. Together, they affect actin dynamics and membrane trafficking. Active Rac1 additionally dephosphorylates/inactivates ERM proteins, consequently causing loss of TLN's anchorage at the cell surface, thus facilitating its internalization. In this way, TLN can no longer act as a brake to the filopodia-to-spine transition, while Rac1 drives local shape changes causing spines to mature. Once internalized, TLN-containing vesicles could theoretically recycle back to the cell surface to reform filopodia, and thereby allow the establishment of new axonal contacts. Alternatively, they can be transported along with flotillin to

Figure 3 Internalization of Telencephalin involves Rac1-mediated actin remodelling, ERM dephosphorylation as well as its release from binding to ERM proteins. (**A**) HeLa cells co-expressing TLN–Cherry and Rac1V12–GFP were stained for surface TLN (blue) in non-permeabilized cells using anti-Cherry antibody to show the internal nature of the TLN-containing vesicles (arrowheads). (**B**) HeLa cells co-expressing untagged TLN (colour-coded: red) and Rac1V12–GFP (colour coded: blue) were incubated with fluorescent dextran beads (70 kDa) (colour coded: green) to assay macropinocytosis. Arrowheads indicate overlap of beads with some of the TLN-positive endosomes. (**C**) HeLa cells co-expressing TLN–Cherry and Rac1V12–GFP were stained for phosphorylated ERM proteins (pERM; blue). Arrowheads indicate internalized TLN, while arrows point out a membrane ruffle where TLN and Rac1 are found colocalizing. Note that the transfected cell displays overall reduced pERM staining and is largely devoid of filopodia and microvilli-like structures. (**D**) Literature-based scheme depicting how GTP-bound ARF6 activates Rac1 by activating its GEF, thereby inducing actin remodelling and membrane trafficking. The active Rac1 mutant (Rac1V12) used in (**A**–**C**) is indicated. Also shown is the Rac1-mediated dephosphorylation/inactivation of ERM proteins, and their subsequent release from binding to plasma membrane proteins, like TLN. Together, these effects lead to the disassembly of filopodia and microvilli-like structures. (**E**) HeLa cell (top panel) and primary hippocampal neuron (DIV 14) (bottom panel) co-expressing TLN–Cherry and VSVG-tagged FERM domain were stained for VSVG (green). Arrowheads indicate TLN- and FERM-containing internal vesicles, while the arrow (bottom panel) indicates their association within a filopodium from where TLN likely internalizes. Bars: 10 μm.

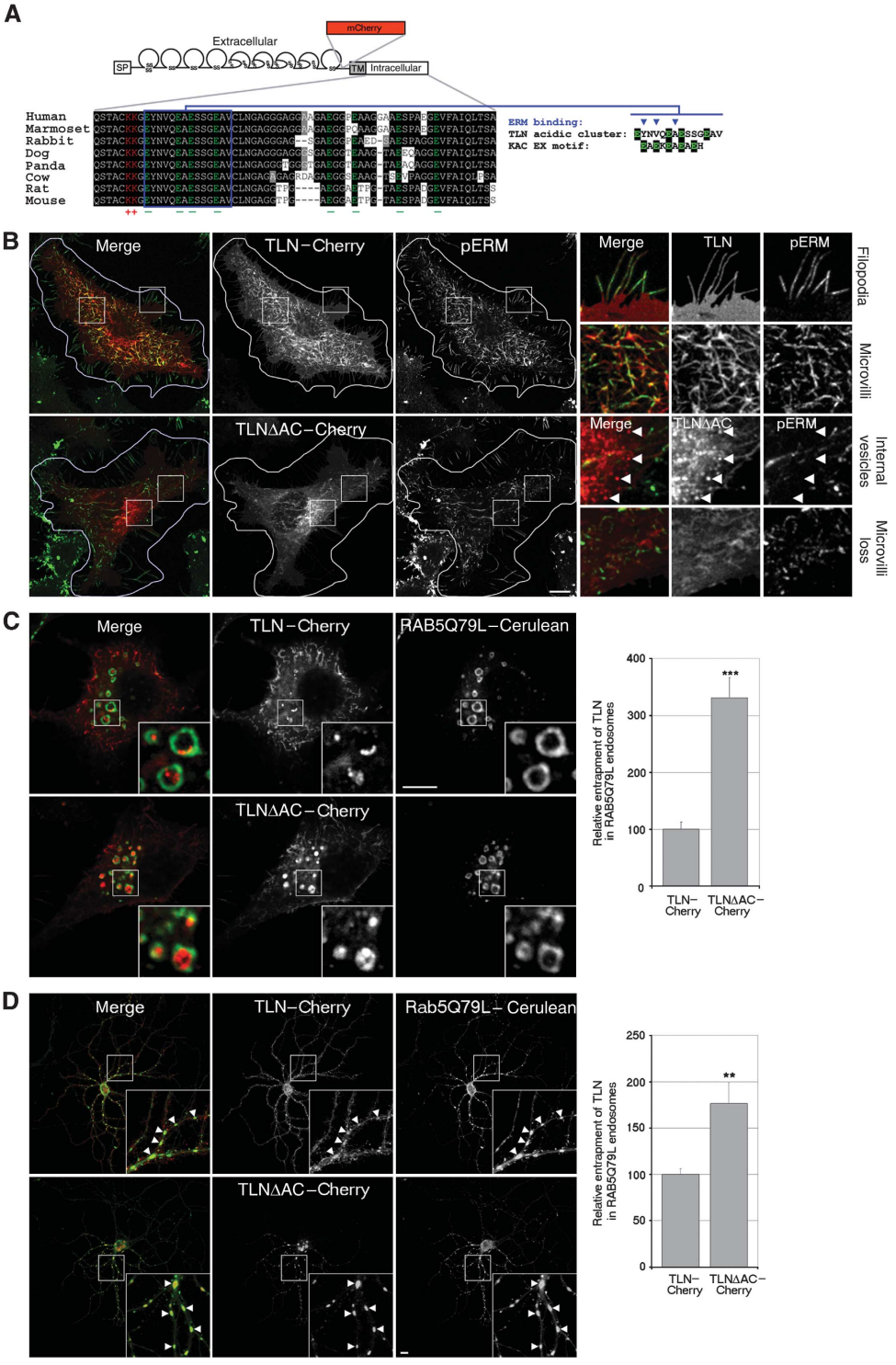

Figure 4 Deletion of an acidic cluster/ERM-binding domain of Telencephalin enhances its internalization. (**A**) Scheme depicting the signal peptide (SP), extra- and intracellular domains of TLN, as well as the position of the internal Cherry tag, proximal to the trans-membrane region (TM). Also shown is the amino-acid sequence of the intracellular domain of human TLN, and its alignment with those from other species. Boxed in blue is a juxta-membrane cluster of acidic residues that fall within a well-conserved region. The residues essential for binding to ERM proteins (blue arrowheads) and the alignment of the TLN acidic cluster with the acidic EX motif of the KAC motif, which is implicated in ARF6-dependent trafficking are also depicted. (**B**) HeLa cells expressing either TLN–Cherry (top panel) or its acidic cluster-deleted mutant (TLNΔAC) (bottom panel) were stained for pERM (green). Insets show that in contrast to full-length TLN, which localizes to pERM-positive filopodia and microvilli-like structures, TLNΔAC is found mostly in internal vesicles. Cells expressing TLNΔAC also have fewer filopodia and microvilli-like structures. (**C**) HeLa cells co-expressing either TLN–Cherry (top panel) or TLNΔAC–Cherry (bottom panel) with RAB5Q79L–Cerulean, fixed at the same time point after transfection. Insets show entrapment of TLN in enlarged RAB5 endosomes, which is more prominent for TLNΔAC than for full-length TLN. Multiple randomly selected cells were analysed and the accompanying quantification is shown in graphs. The obtained means ± s.e.m. values were expressed relative to full-length TLN, which was defined as 100% (TLN: 100.0 ± 12.9; TLNΔAC: 331.3 ± 35.3). (**D**) As in (**C**) but studied in hippocampal neurons (DIV 14). The values are TLN: 100.0 ± 6.4 and TLNΔAC: 176.5 ± 22.4. Arrowheads indicate entrapment of TLN in Rab5Q79L endosomes. Note that, in contrast to TLNΔAC, full-length TLN is still evidently visible at the cell surface. *P*-values (Student's *t*-test): $^{**}P<0.01$, $^{***}P<0.001$. Bars: 10 μm.

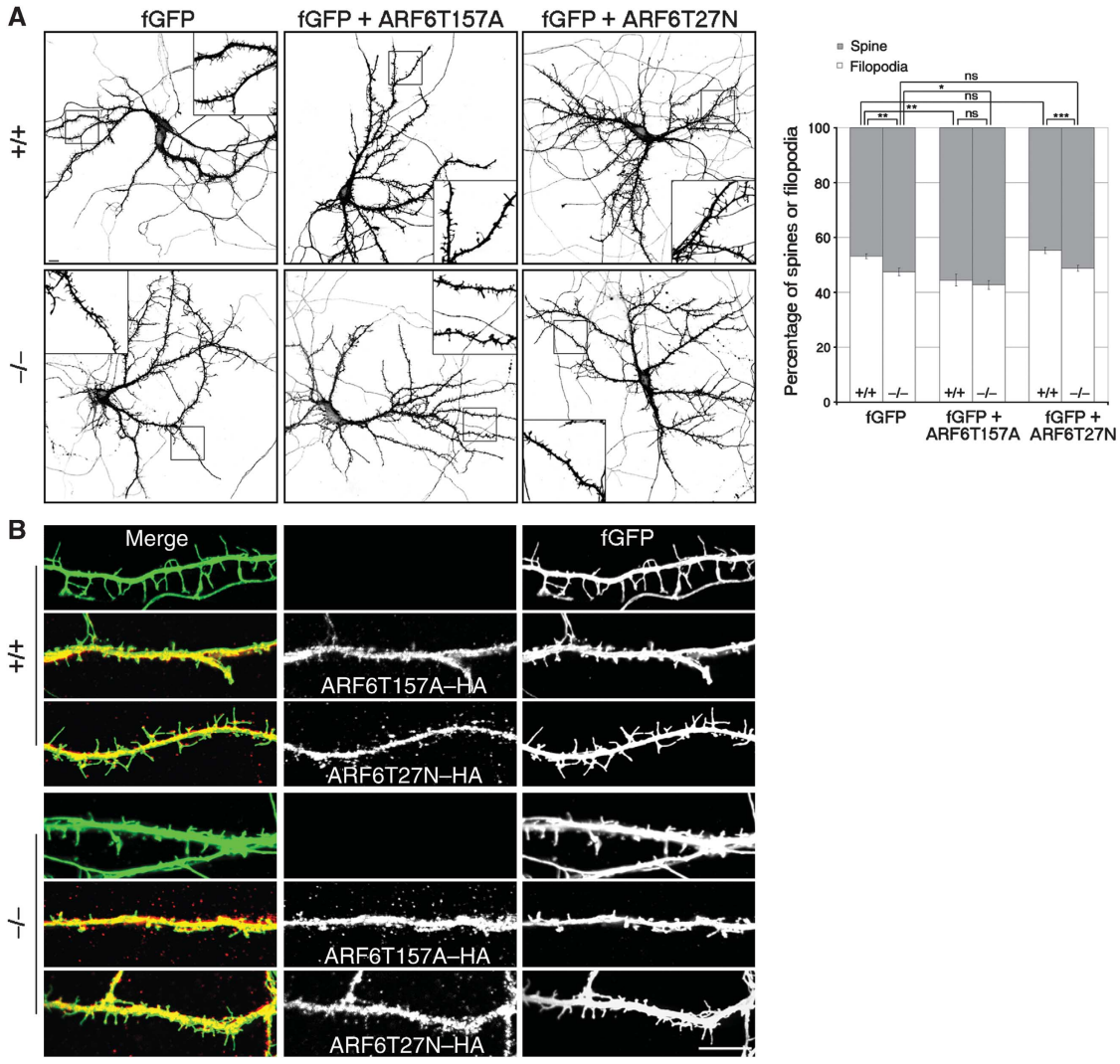

Figure 5 ARF6-mediated promotion of spine development is reduced in hippocampal neurons deficient for Telencephalin. (**A**) Primary hippocampal neurons (DIV 13) expressing farnesylated GFP (fGFP) (to visualize membrane structures) alone or together with ARF6T157A–HA or ARF6T27N–HA for 48 h were analysed in wild-type (+/+) and TLN-deficient (−/−) neurons. Insets show dendritic protrusions. Acquired images were subjected to morphometric analysis as described in Materials and methods. For $TLN^{+/+}$ neurons, depicted in graphs spine percentages are fGFP alone (46.9 ± 0.9), fGFP + ARF6T157A (55.6 ± 2.2) and fGFP + ARF6T27N (44.7 ± 1.3). For $TLN^{-/-}$ neurons, spine percentages are fGFP alone (52.6 ± 1.4), fGFP + ARF6T157A (57.3 ± 1.6) and fGFP + ARF6T27N (51.2 ± 1.2). Note that $TLN^{+/+}$ neurons expressing ARF6T157A show a significant increase in number of spines when compared to fGFP expressing control. This is also the case in $TLN^{-/-}$ neurons, but here the observed relative difference is less apparent: 4.7 versus 8.7% in $TLN^{-/-}$ and $TLN^{+/+}$ neurons, respectively. Note also that $TLN^{-/-}$ neurons expressing fGFP alone show significantly more spines (less filopodia) when compared to fGFP expressing wild-type neurons. Data were collected from 400 to 1400 protrusions on dendrites of 6–8 neurons in three independent experiments. (**B**) Representative images of dendritic sections as described in (**A**). Note the more prominent presence of spine structures in both $TLN^{-/-}$ and wild-type neurons when ARF6T157A (activated) mutant is expressed. *P*-values (Student's *t*-test): $*P<0.05$; $**P<0.01$; $***P<0.001$; NS: no significant difference. Bars: 10 μm.

CD63-containing MVBs for degradation/exosomal release. In well-developed neurons, however, both proteins, likely under certain (stress) conditions, can end up with TLN in aberrant intracellular vacuoles (Esselens *et al*, 2004), implying their involvement in a related trafficking pathway.

(In)activation of ARF6, Rac1 and ERMs: lessons from immunological synapses

Although the involvement of ARF6, and its activator, EFA6A, in spine morphogenesis was demonstrated to depend on Rac1 (Choi *et al*, 2006), the underlying mechanism remained unclear. In separate studies, induction of spine morphogenesis in neurons was shown to depend on recruitment and activation of the Rac1 activator, Kalirin (Penzes *et al*, 2003), while in HeLa cells both the recruitment and the activation were shown to be mediated by ARF6 (Koo *et al*, 2007). Noteworthy, endogenous TLN and Kalirin can be found within the same dendritic protrusions (Supplementary Figure S19). However, unlike its association with EFA6A (Figure 1), TLN's more prominent colocalization with Kalirin occurs in mature neurons and seems to coincides with the beginning of a spine maturation process (Supplementary Figure S19). This agrees with the study of Penzes *et al* (2003) and our working model, whereby EFA6A

would have an initiating role in this process, while its downstream targets, including ARF6, Kalirin and Rac1 would require appropriate triggering for their recruitment to sites of maturing spines (synapses).

Interestingly, Rac1 was shown to participate in morphological changes also during immunological synapse formation in a dual way. First, by inactivating/dephosphorylating ERM proteins, it creates flexible regions of the plasma membrane

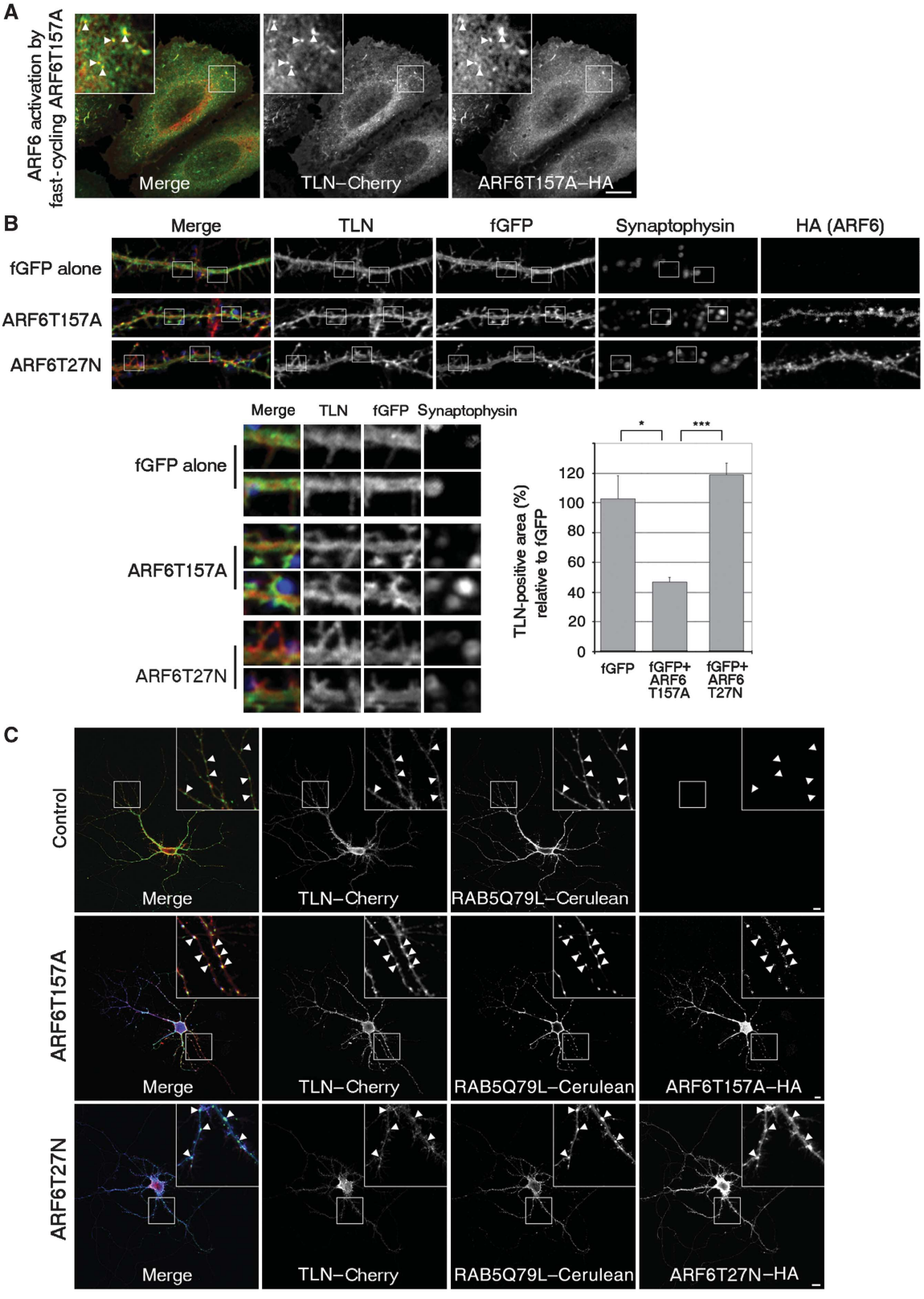

by disanchoring the actin cytoskeleton from the membrane. Second, by increasing actin polymerization it creates ruffles/lamellipodia that enhance binding and scanning for appropriate ligands (Faure *et al*, 2004; Nijhara *et al*, 2004). A very similar situation could be envisioned in the transition of filopodia to spines during neuronal synapse formation. In such a scenario, upon establishment of a contact with the axon, maybe through binding of TLN to presynaptic integrins, like LFA1 (Wakabayashi *et al*, 2008), a known ligand of TLN (Mizuno *et al*, 1997; Tian *et al*, 1997), a cascade of events could be triggered including activation/recruitment of EFA6A, ARF6, Kalirin and finally Rac1. Rac1 activation would then work as in immunological synapses, only now by regulating the internalization of TLN, as well as actin remodelling, both of which would promote the formation of mushroom-shaped spines. As our data, using $TLN^{-/-}$ primary hippocampal neurons, show a significant, yet only partial contribution of TLN in this ARF6-mediated process, involvement of other (adhesion) molecules cannot be excluded. The ultimate morphological outcome in such a working model would thus depend on an integration of a number of factors, including internalization and recycling events of the key proteins.

Parallels between the immunological and neuronal synapse have indeed been made before, however, in a different perspective (Matsuno *et al*, 2006; Gahmberg *et al*, 2008; Tian *et al*, 2009). In fact, another member of the ICAM family, namely ICAM1, is expressed in lymphocytes, and like TLN, binds LFA1. Interestingly, ICAM1 has been identified as a novel ARF6-cargo protein in a recent proteomic screen (Eyster *et al*, 2009) and like TLN and other ICAMs it interacts with ERM proteins at the cell surface (Bretscher *et al*, 2002).

Flotillin, lipid rafts and TLN-mediated filopodia formation

Flotillin is a lipid raft protein (Bickel *et al*, 1997), and interestingly, synapse formation has been shown to be promoted by lipid rafts, mainly through the action of glia-derived and neuronal-synthesized cholesterol (Mauch *et al*, 2001; Suzuki *et al*, 2007). ARF6-mediated endocytosis has also been described to require cholesterol (Naslavsky *et al*, 2004), and trafficking of lipid rafts may be regulated by ARF6, as shown during adhesion-dependent signalling (Balasubramanian *et al*, 2007). A further similarity between ARF6 and flotillin is that both are believed to modulate several cell surface-associated activities, including cell-cell adhesion and migration (D'Souza-Schorey and Chavrier, 2006; Stuermer, 2010). They also both regulate trafficking of CD59, a GPI-anchored protein that resides in lipid rafts (Naslavsky *et al*, 2004; Glebov *et al*, 2006).

In our experiments, TLN and flotillin associate closely, both intracellularly (within the same vesicles), as well as at specific cell surface microdomains with a distinct patchy appearance, found at the neuronal cell body. These microdomains appear to extend along the dendritic shaft and filopodia at a smaller scale, where they could act as platforms for internalization and recycling events, involving TLN and other proteins. This could in turn influence filopodia formation/spine morphogenesis. Interestingly, flotillin2 was shown to promote filopodia formation in HeLa cells (Neumann-Giesen *et al*, 2004), and a recent study in hippocampal neurons demonstrated that flotillin1 promotes specifically glutamatergic, but not GABAergic, synapse formation (Swanwick *et al*, 2010b). Coincidentally, expression of TLN is confined to these excitatory neurons (Benson *et al*, 1998). As flotillin is a lipid raft protein, it may promote filopodia formation by locally altering the plasma-membrane composition, and thereby membrane tension, thus facilitating initial protrusion of filopodia. In fact, this same mechanism likely accounts for the increased neurite branching induced by flotillin expression (Swanwick *et al*, 2010a), and correlates well with the high TLN expression levels in well-arborized neurons (Benson *et al*, 1998). Noteworthy, ARF6 has also been shown to regulate neurite branching (Hernández-Deviez *et al*, 2002).

Trafficking of TLN to CD63-containing late endosomes/MVBs

TLN colocalizes with CD63-containing MVBs in HeLa cells and neurons (both at the cell body and to a lesser extent along the dendrites). These endosomes are likely destined for lysosomal degradation, however, another possibility is that they may also be recycled back to the plasma membrane where the ILVs could be released as exosomes. This in turn, would enable a new way of communication of TLN with the extracellular environment, potentially important (1) for proper establishment of axonal contacts, by guiding LFA1-expressing axons (Wakabayashi *et al*, 2008) to filopodia; (2) for dendritic filopodia formation, which is promoted by homophilic interactions of TLN (Tian *et al*, 2007); and (3) during inflammation, to sensitize and guide the migration of LFA1-expressing microglia to affected neurons, much like how antigen-presenting cells secrete ICAM1-containing exosomes to stimulate immune responses (Théry *et al*, 2002; Segura *et al*, 2005).

Figure 6 Internalization of Telencephalin is coupled to ARF6-mediated promotion of spine development. (**A**) HeLa cells co-expressing TLN–Cherry and the fast-cycling (active) ARF6T157A–HA mutant were stained for HA (green). Arrowheads indicate intracellular vesicles where both proteins are found colocalizing. (**B**) Wild-type hippocampal neurons (DIV 13) expressing fGFP (to visualize membrane periphery) alone or together with ARF6T157A–HA or (inactive) ARF6T27N–HA. Neurons were stained for HA to check for ARF6 expression, synaptophysin (blue) to control for synaptic density, and TLN (red) to determine its relative distribution (surface versus internal) along dendrites. Note that in neurons expressing ARF6T157A, TLN staining appears more centrally localized within the dendritic shaft compared to neurons expressing fGFP alone (control) or together with ARF6T27N. This was confirmed through the quantitative threshold analysis of acquired images that revealed a significant decrease in the relative area containing endogenous TLN as compared to fGFP. The obtained percentages depicted in the graph are fGFP alone: 102.7 ± 15.4; fGFP + ARF6T157A: 46.7 ± 3.1; fGFP + ARF6T27N: 118.8 ± 7.8. Data were collected from multiple dendritic sections of several different neurons. (**C**) Hippocampal neurons (DIV 13) co-expressing TLN–Cherry and RAB5Q79L–Cerulean (green) alone or together with ARF6T157A–HA or ARF6T27N–HA were stained for HA (colour coded: blue). Arrowheads show more prominent entrapment of TLN in RAB5Q79L endosomes in neurons expressing ARF6T157A when compared to those expressing ARF6T27N or no ARF6 mutant. Neurons were fixed at the same time point after transfection. The data indicate that ARF6 activation can induce TLN internalization. *P*-values (Student's *t*-test): $^{*}P<0.05$; $^{***}P<0.001$. Bars: 10 μm.

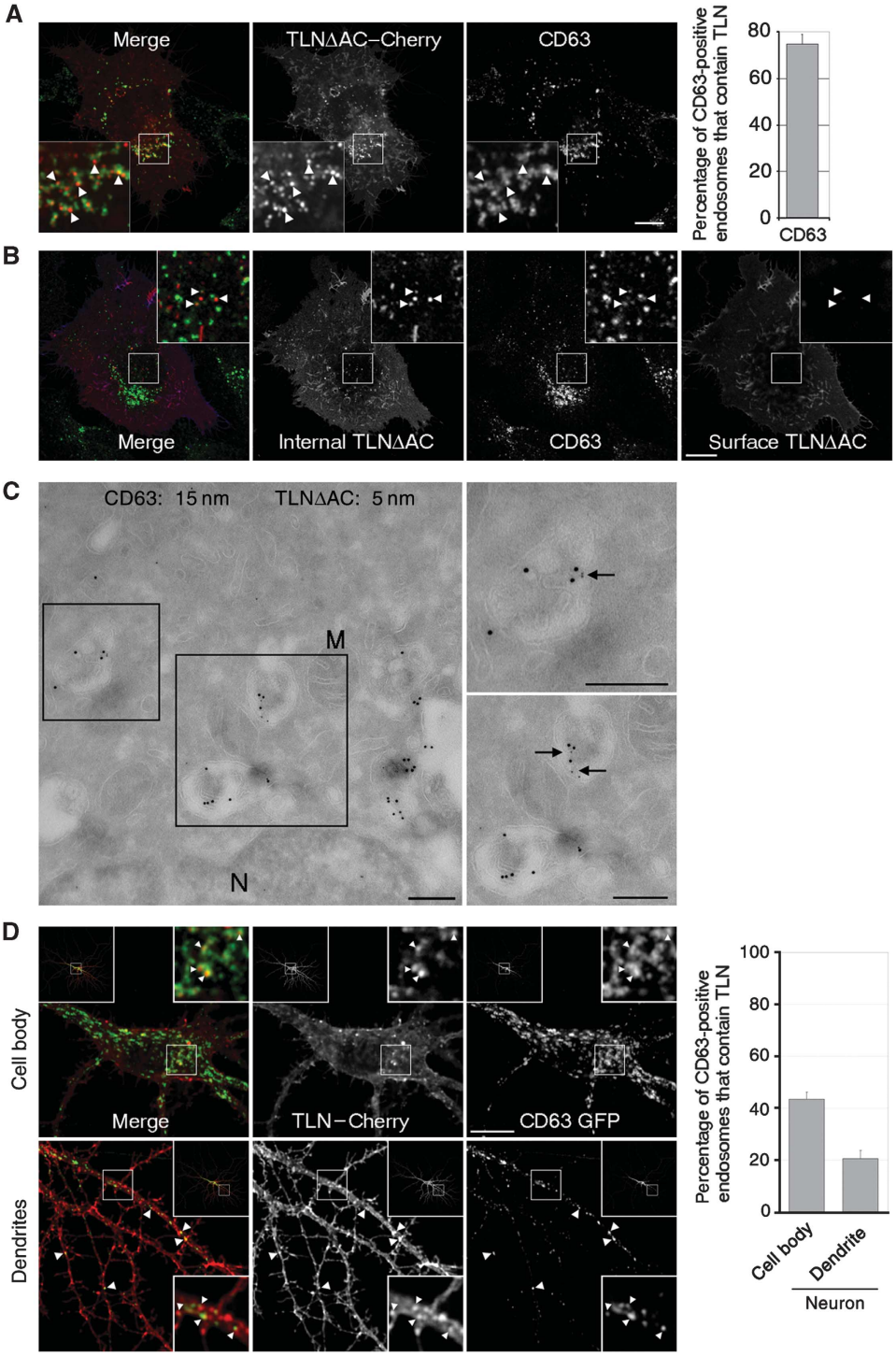

Figure 7 Internalized Telencephalin is routed to CD63-positive multivesicular bodies. (**A**) HeLa cells expressing TLNΔAC–Cherry were stained for endogenous CD63 (green). Arrowheads indicate juxta-positioning of TLN and CD63. The percentage of CD63-positive endosomes that contain TLNΔAC is shown in the graph. Quantifications were made using multiple, randomly selected cells, and the obtained percentage and s.e.m. value are 74.8 ± 4.2. (**B**) Antibody uptake assay using HeLa cells expressing TLNΔAC–Cherry (2-h uptake). Arrowheads indicate internalized TLNΔAC (red) within CD63- (green) positive endosomes. Surface TLNΔAC (blue) was stained for before cell permeabilization. (**C**) Immuno-EM micrograph of a HeLa cell expressing TLNΔAC–Cherry, stained for TLNΔAC (5 nm) and CD63 (15 nm). Arrows show intralumenal vesicles, where TLNΔAC and CD63 are closely apposed. M: mitochondria, N: nucleus. Bar: 200 nm. (**D**) Hippocampal neuron (DIV 13) co-expressing TLN–Cherry and CD63-GFP. Arrowheads indicate the juxta-positioning of TLN and CD63 both at the cell body (top panel), and along the dendrites (bottom panel). The extent of colocalization was quantified like in (**A**). The obtained percentages and s.e.m. values depicted in graphs are 43.5 ± 2.7 (cell body) and 20.5 ± 3.1 (dendrites). Bars: 10 μm, unless otherwise indicated.

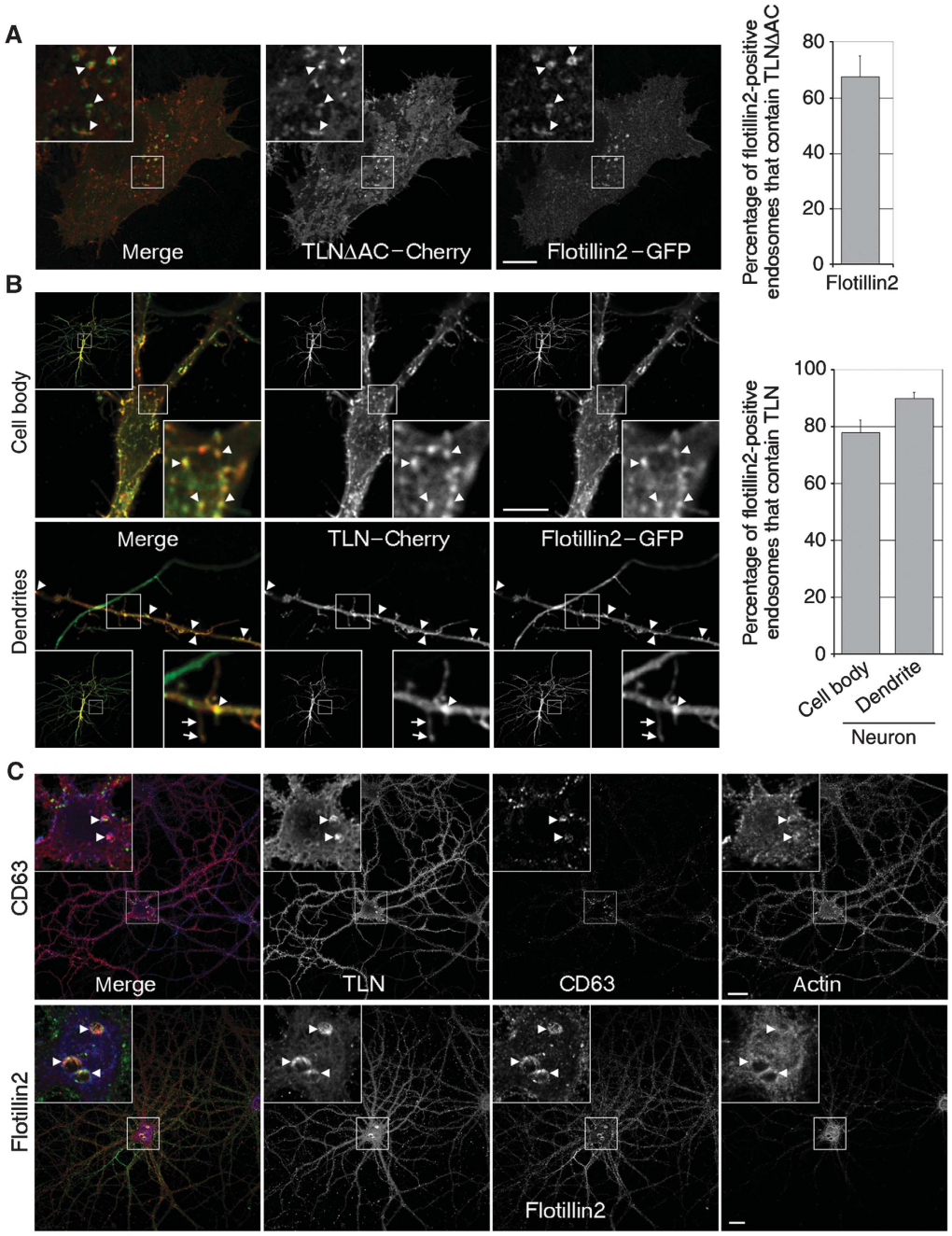

Figure 8 Internalized Telencephalin co-trafficks with flotillin and can co-accumulate intracellularly with it and CD63. (**A**) HeLa cells co-expressing TLNΔAC–Cherry and flotillin2–GFP. Arrowheads indicate the juxta-positioning of both proteins at internal vesicles. The percentage of flotilin2-GFP endosomes that contain TLNΔAC is shown in the graph. Quantifications were made using multiple, randomly selected cells, and the obtained percentage and s.e.m. value are 67.7 ± 7.5. (**B**) Hippocampal neuron (DIV 13) co-expressing TLN–Cherry and flotillin2–GFP. Arrowheads indicate the internal colocalization of TLN and flotilin2 at the cell body (top panel), and along the dendrites (bottom panel). The extent of colocalization was quantified like in (**A**). The obtained percentages and s.e.m. values depicted in graphs are 78.0 ± 4.4 (cell body) and 90.0 ± 2.2 (dendrites). Arrows indicate the presence of both proteins at filopodia from where they likely co-internalize. (**C**) Well-developed hippocampal neurons (DIV 26) were stained for endogenous TLN (red), actin (blue) and CD63 (top panel, green) or flotillin2 (bottom panel, green). Arrowheads indicate colocalization of endogenous CD63 and flotillin2 with TLN in intracellular accumulations. Bar: 10 μm.

We previously showed that TLN trafficking is altered in PSEN1-deficient hippocampal neurons, and to a lesser degree in well-developed wild-type neurons, where TLN accumulates intracellularly in autophagic-like vacuoles (Esselens *et al*, 2004). Recently, a convergence of autophagic and CD63-containing degradation routes was revealed (Fader *et al*, 2008; 2009), suggesting that the TLN-CD63 positive organelles observed in older neurons may reflect an initiation of transport jamming or delayed degradation, an aspect that requires further investigation.

Taken together, we provide a novel mechanism how TLN trafficking affects the filopodia-to-spine transition in hippocampal neurons. Whereas its surface presence/function is largely determined by ARF6-mediated internalization/sorting

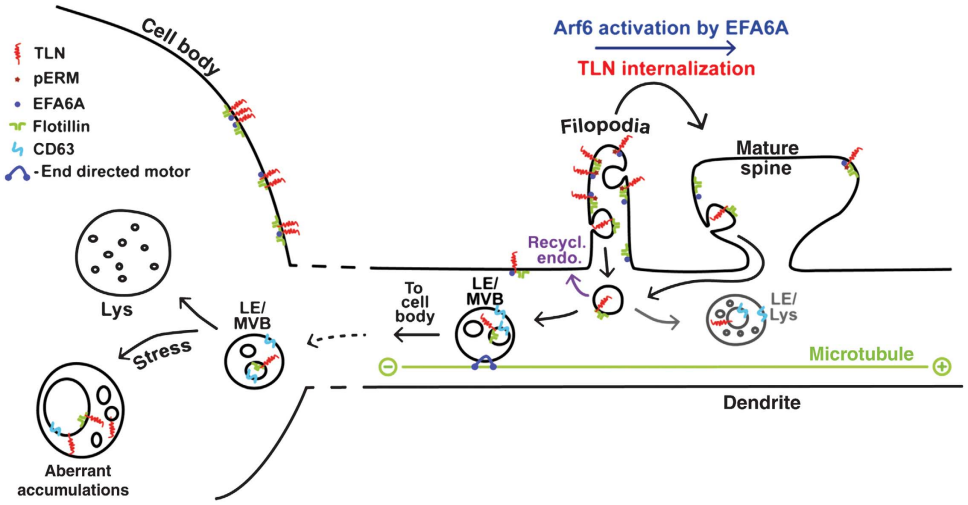

Figure 9 Proposed model of Telencephalin trafficking in hippocampal neurons and its implications for spine morphogenesis. Within filopodia, EFA6A associates with TLN at defined membrane subdomains that contain flotillin. After getting triggered it activates ARF6, which indirectly activates Rac1 (not shown), thereby affecting actin dynamics and membrane trafficking. Active Rac1 dephosphorylates and inactivates ERM proteins. This causes TLN to lose its anchorage at the surface and facilitates its internalization. Concomitant with its endocytosis, Rac1 drives shape changes through actin polymerization, thus causing filopodia to mature into spines. Once internalized, TLN-containing vesicles in the dendritic shaft may be either recycled (recycling endo) back to the cell surface, to reform filopodia and to establish new axonal contacts. Alternatively they are transported along with flotillin to CD63-containing late endosomal/multivesicular bodies (LE/MVBs) found either locally in dendritic shafts, or within the cell body. Part of this pathway may become altered under certain (stress) conditions in well-developed neurons causing TLN to accumulate aberrantly together with CD63 and flotillin in intracellular autophagic-like vacuoles (as observed in younger PSEN1$^{-/-}$ neurons; Esselens *et al*, 2004).

events, later intracellular routing of TLN involves both the lipid raft marker protein, flotillin and targeting to CD63-positive late endosomes. These findings extend the known role of ARF6 in dendritic spine morphogenesis by implying its involvement in the regulated internalization of a major dendritic adhesion molecule, TLN. So far, TLN is the only known adhesion molecule executing a negative regulation on spine maturation. By demonstrating that TLN functionally interacts with ARF6 via EFA6A, we now show that the function of ARF6 in positively regulating spine maturation is at least in part mediated through the downregulation of TLN surface expression in dendritic filopodia. Interestingly, TLN-deficient neurons display larger spine heads than neurons from wild-type mice suggesting an additional role of TLN in refinement of functional neuronal circuits in telencephalon, with potential impact on higher brain functions (Matsuno *et al*, 2006). This puts our findings in a physiologically relevant context of learning and memory acquisition and shows that insights into TLN's trafficking could open up novel avenues that would allow the modulation of its function in spine morphogenesis. This is of pivotal importance during development (Barkat *et al*, 2011), as well as later into adulthood (Nakamura *et al*, 2001).

Materials and methods

Cell culture, transfection and cell-based assays

HeLa cells were transfected using FuGENE 6 (Roche Diagnostics) in a reverse transfection procedure. The culture of primary hippocampal neurons has been described previously (Esselens *et al*, 2004; Kaech and Banker, 2006). Neurons were transfected using Lipofectamine 2000 (Invitrogen) or calcium phosphate precipitation method (Köhrmann *et al*, 1999). All the transfection experiments lasted between 24 and 72 h depending on the experimental setting. TLN$^{-/-}$ mice were provided by Y Furutani and Y Yoshihara (Riken, Wako, Japan). Macropinocytosis was assayed using fluorescent dextran beads (70 kDa; 1 mg/ml) that were incubated with cells for 1 h, and subsequently washed out prior to fixation and staining. Details regarding the antibody uptake assays, the detergent-based extraction procedure, as well as information on the used constructs/antibodies can be found in Supplementary data.

Co-immunoprecipitation and western blot analysis

Transfected HeLa cells were lysed in ice-cold lysis buffer (10 mM TrisCl (pH 8), 1% NP40, 100 mM NaCl, complemented with protease inhibitors and 1 mM Pefabloc; Roche Diagnostics) for 30 min, and cleared by centrifugation (13 000 *g*, 15 min). Immunoprecipitates were collected (4000 *g*, 1 min) after incubating the supernatant (250 μg protein diluted with lysis buffer without NP-40) with 6 μg/ml rabbit anti-GFP (Invitrogen) or anti-TLN (B36.1) antibody overnight at 4°C, followed by addition of Protein A Plus Agarose (30 μl, Thermo-Scientific) for 4 h at 4°C. The beads were subsequently washed in lysis buffer with higher salt (400 mM NaCl), and thereafter with 0.3 × TBS. The bound proteins were eluted and separated by SDS–PAGE (4–12%) Bis-Tris NuPAGE gels (Invitrogen). Samples were processed for western blotting and immunodetection, while the Western Lightning-Plus ECL reagent (Perkin-Elmer) and AIDA Image Analyzer were used for protein band visualization/intensity quantification, respectively.

Confocal microscopy and immunofluorescence

HeLa cells and hippocampal neurons that were plated on glass coverslips were fixed in (4% paraformaldehyde/4% sucrose in PBS, 20 min or in −20°C methanol, 5 min), permeabilized (0.1% Triton X-100 in PBS, 5 min), blocked (2% BSA, 2% FBS and 1% gelatin in PBS supplemented with 5% serum, incubated with primary antibody (4°C, overnight), washed (PBS), incubated with fluorophore conjugated secondary antibody (RT, 1 h), rinsed, and mounted in Mowiol-containing medium. Alexa-conjugated phalloidin (Invitrogen) was used to label filamentous actin. The secondary antibodies were conjugated with the following fluorophores: Alexa-488, -568, -647 and Pacific Blue (Invitrogen). Images were captured on a confocal (Radiance 2100; Carl Zeiss) connected to an upright microscope (Eclipse E800; Nikon) and using an oil-immersion plan Apo 60 × A/1.40 NA objective lens. Final processing was done using Lasersharp 2000 and Photoshop (Adobe) and restricted to

limited linear colour balance adjustments to interpret merged pictures.

Image analysis and quantification

Morphometric measurements were performed using Imaris image analysis software (Bitplane Scientific Software, Zurich). Neurons were selected randomly, and aspiny interneurons were excluded from the analysis. To determine the percentage of spines or filopodia, spines were defined as dendritic protrusions of 0.4–3 μm length (with or without a head) and filopodia as dendritic protrusions of 3–10 μm in length, as previously described (Choi *et al*, 2006). The percentages of protrusions were grouped (filopodia versus spines) and averaged. Multiple individual neurons were analysed to obtain a population mean.

For the analysis of the presence of endogenous TLN within the dendrite (surface versus internal), acquired images of dendritic sections (40 μm) were processed using ImageJ software (NIH) set for Auto thresholding using the Minimum Method. The obtained data reflect area percentages of the TLN distribution relative to that of fGFP. For fGFP, the percentage defines the complete dendritic area, as it is homogenously distributed and limited to the membrane periphery. For TLN, the area percentages differed, as TLN's distribution varied depending on its internalization. Multiple images of dendrites from independent neurons were analysed to obtain a population mean.

To quantify TLN entrapment in RAB5Q79L endosomes acquired images were analysed using ImageJ software. The relative levels of internalized TLN (TLNΔAC) were compared by dividing its fluorescence intensity, confined to Rab5Q79L endosomes, by its total cell fluorescence. The reported differences were observed in at least three independent experiments and quantified in multiple, randomly selected cells.

For the endosomal overlap analysis, vesicles that stained positive for CD63 or flotillin were scored for the presence/absence of TLN. The percentages of vesicles containing both proteins were calculated. Means from multiple individual cells were averaged to obtain a population mean.

For the microdomain overlap analysis between TLN and EFA6A or flotillin2 at the cell body of neurons, acquired images were processed in ImageJ using the JACop method (Bolte and Cordelières, 2006).

For all data analysis, the two-tailed Student's *t*-test was used to compare the mean ± s.e.m. values. The details regarding the ARF6 knockdown experimental setting and quantification of the observed phenomena can be found in Supplementary data.

Supplementary data

Supplementary data are available at *The EMBO Journal* Online (http://www.embojournal.org).

Acknowledgements

We gratefully acknowledge the following scientists who provided expression vectors and antibodies: Janis Burkhardt, Philippe Chavrier, Julie Donaldson, Eunjoon Kim, Judith Klumperman, Lawrence Rajendran, Roger Tsien, Betty Eipert and Marino Zerial. We wish to particularly thank Yutaka Furutani, Yoshihiro Yoshihara (Riken Brain Science Institute, Wako, Japan) and Masayoshi Mishina (Univ. Tokyo, Japan) for providing us with the TLN$^{-/-}$ mice. We thank Maria Francesca Baietti for helpful comments, and Sebastian Munck for help with the Imaris software. This work was financially supported by the VIB, and grants from the Research Foundation Flanders (FWO; G.0663.09 and G.0754.10), and KU Leuven (GOA/11/009)/Hercules Foundation (AKUL/09/037), the Stichting Alzheimer Onderzoek SAO-FRMA (grant cycle 2010), the federal government (IAP P6/43 and P7/2012-2017) and the Alzheimer Association (IIRG-08-91535). TR held postdoctoral fellowships from the FWO and KU Leuven, and RS obtained a Marie-Curie postdoctoral fellowship. AP is supported by an FWO PhD fellowship.

Author contributions: The study was conceived and supervised by TR and WA; TR and AP performed most of the experiments. ID, VB, and CM contributed with biochemical and cell culture assays. PB contributed with EM analysis. TR wrote the initial manuscript and TR, AP, RS and WA edited the manuscript.

Conflict of interest

The authors declare that they have no conflict of interest.

References

Allenspach EJ, Cullinan P, Tong J, Tang Q, Tesciuba AG, Cannon JL, Takahashi SM, Morgan R, Burkhardt JK, Sperling AI (2001) ERM-dependent movement of CD43 defines a novel protein complex distal to the immunological synapse. *Immunity* **15:** 739–750

Amieva MR, Litman P, Huang L, Ichimaru E, Furthmayr H (1999) Disruption of dynamic cell surface architecture of NIH3T3 fibroblasts by the N-terminal domains of moesin and ezrin: *in vivo* imaging with GFP fusion proteins. *J Cell Sci* **112,** Part 1 111–125

Annaert WG, Esselens C, Baert V, Boeve C, Snellings G, Cupers P, Craessaerts K, De Strooper B (2001) Interaction with telencephalin and the amyloid precursor protein predicts a ring structure for presenilins. *Neuron* **32:** 579–589

Balasubramanian N, Scott D, Castle J, Casanova J, Schwartz M (2007) Arf6 and microtubules in adhesion-dependent trafficking of lipid rafts. *Nat Cell Biol* **9:** 1381–1391

Barkat TR, Polley DB, Hensch TK (2011) A critical period for auditory thalamocortical connectivity. *Nat Neurosci* **14:** 1189–1194

Benson DL, Yoshihara Y, Mori K (1998) Polarized distribution and cell type-specific localization of telencephalin, an intercellular adhesion molecule. *J Neurosci Res* **52:** 43–53

Bickel PE, Scherer PE, Schnitzer JE, Oh P, Lisanti MP, Lodish HF (1997) Flotillin and epidermal surface antigen define a new family of caveolae-associated integral membrane proteins. *J Biol Chem* **272:** 13793–13802

Bolte S, Cordelières FP (2006) A guided tour into subcellular colocalization analysis in light microscopy. *J Microsc* **224**(Part 3): 213–232

Bretscher A, Edwards K, Fehon RG (2002) ERM proteins and merlin: integrators at the cell cortex. *Nat Rev Mol Cell Biol* **3:** 586–599

Brown FD, Rozelle AL, Yin HL, Balla T, Donaldson JG (2001) Phosphatidylinositol 4,5-bisphosphate and Arf6-regulated membrane traffic. *J Cell Biol* **154:** 1007–1017

Choi S, Ko J, Lee JR, Lee HW, Kim K, Chung HS, Kim H, Kim E (2006) ARF6 and EFA6A regulate the development and maintenance of dendritic spines. *J Neurosci* **26:** 4811–4819

D'Souza-Schorey C, Chavrier P (2006) ARF proteins: roles in membrane traffic and beyond. *Nat Rev Mol Cell Biol* **7:** 347–358

D'Souza-Schorey C, van Donselaar E, Hsu VW, Yang C, Stahl PD, Peters PJ (1998) ARF6 targets recycling vesicles to the plasma membrane: insights from an ultrastructural investigation. *J Cell Biol* **140:** 603–616

de Gassart A, Geminard C, Fevrier B, Raposo G, Vidal M (2003) Lipid raft-associated protein sorting in exosomes. *Blood* **102:** 4336–4344

De Strooper B, Annaert W (2010) Novel research horizons for presenilins and γ-secretases in cell biology and disease. *Annu Rev Cell Dev Biol* **26:** 235–260

Decressac S, Franco M, Bendahhou S, Warth R, Knauer S, Barhanin J, Lazdunski M, Lesage F (2004) ARF6-dependent interaction of the TWIK1 K+ channel with EFA6, a GDP/GTP exchange factor for ARF6. *EMBO Rep* **5:** 1171–1175

Donaldson JG, Porat-Shliom N, Cohen LA (2009) Clathrin-independent endocytosis: a unique platform for cell signaling and PM remodeling. *Cell Signal* **21:** 1–6

Esselens C, Oorschot V, Baert V, Raemaekers T, Spittaels K, Serneels L, Zheng H, Saftig P, De Strooper B, Klumperman J, Annaert W (2004) Presenilin 1 mediates the turnover of telencephalin in hippocampal neurons via an autophagic degradative pathway. *J Cell Biol* **166:** 1041–1054

Eyster CA, Higginson JD, Huebner R, Porat-Shliom N, Weigert R, Wu WW, Shen RF, Donaldson JG (2009) Discovery of new cargo proteins that enter cells through clathrin-independent endocytosis. *Traffic* **10:** 590–599

Fader C, Colombo M (2009) Autophagy and multivesicular bodies: two closely related partners. *Cell Death Differ* **16:** 70–78

Fader C, Sánchez D, Furlán M, Colombo M (2008) Induction of autophagy promotes fusion of multivesicular bodies with autophagic vacuoles in k562 cells. *Traffic* **9:** 230–250

Faure S, Salazar-Fontana LI, Semichon M, Tybulewicz VL, Bismuth G, Trautmann A, Germain RN, Delon J (2004) ERM proteins regulate cytoskeleton relaxation promoting T cell-APC conjugation. *Nat Immunol* **5:** 272–279

Franco M, Peters PJ, Boretto J, van Donselaar E, Neri A, D'Souza-Schorey C, Chavrier P (1999) EFA6, a sec7 domain-containing exchange factor for ARF6, coordinates membrane recycling and actin cytoskeleton organization. *EMBO J* **18:** 1480–1491

Furutani Y, Matsuno H, Kawasaki M, Sasaki T, Mori K, Yoshihara Y (2007) Interaction between telencephalin and ERM family proteins mediates dendritic filopodia formation. *J Neurosci* **27:** 8866–8876

Gahmberg CG, Tian L, Ning L, Nyman-Huttunen H (2008) ICAM-5–a novel two-facetted adhesion molecule in the mammalian brain. *Immunol Lett* **117:** 131–135

Glebov OO, Bright NA, Nichols BJ (2006) Flotillin-1 defines a clathrin-independent endocytic pathway in mammalian cells. *Nat Cell Biol* **8:** 46–54

Gong Q, Weide M, Huntsman C, Xu Z, Jan LY, Ma D (2007) Identification and characterization of a new class of trafficking motifs for controlling clathrin-independent internalization and recycling. *J Biol Chem* **282:** 13087–13097

Grant BD, Donaldson JG (2009) Pathways and mechanisms of endocytic recycling. *Nat Rev Mol Cell Biol* **10:** 597–608

Hernández-Deviez D, Casanova J, Wilson J (2002) Regulation of dendritic development by the ARF exchange factor ARNO. *Nat Neurosci* **5:** 623–624

Kaech S, Banker G (2006) Culturing hippocampal neurons. *Nat Protoc* **1:** 2406–2415

Kaufmann WE, Moser HW (2000) Dendritic anomalies in disorders associated with mental retardation. *Cereb Cortex* **10:** 981–991

Knafo S, Alonso-Nanclares L, Gonzalez-Soriano J, Merino-Serrais P, Fernaud-Espinosa I, Ferrer I, DeFelipe J (2009) Widespread changes in dendritic spines in a model of Alzheimer's disease. *Cereb Cortex* **19:** 586–592

Köhrmann M, Haubensak W, Hemraj I, Kaether C, Lessmann VJ, Kiebler MA (1999) Fast, convenient, and effective method to transiently transfect primary hippocampal neurons. *J Neurosci Res* **58:** 831–835

Koo TH, Eipper BA, Donaldson JG (2007) Arf6 recruits the Rac GEF Kalirin to the plasma membrane facilitating Rac activation. *BMC Cell Biol* **8:** 29

Ledesma MD, Simons K, Dotti CG (1998) Neuronal polarity: essential role of protein-lipid complexes in axonal sorting. *Proc Natl Acad Sci USA* **95:** 3966–3971

Matsuno H, Okabe S, Mishina M, Yanagida T, Mori K, Yoshihara Y (2006) Telencephalin slows spine maturation. *J Neurosci* **26:** 1776–1786

Matus A (2000) Actin-based plasticity in dendritic spines. *Science* **290:** 754–758

Mauch DH, Nägler K, Schumacher S, Göritz C, Müller EC, Otto A, Pfrieger FW (2001) CNS synaptogenesis promoted by glia-derived cholesterol. *Science* **294:** 1354–1357

Mizuno T, Yoshihara Y, Inazawa J, Kagamiyama H, Mori K (1997) cDNA cloning and chromosomal localization of the human telencephalin and its distinctive interaction with lymphocyte function-associated antigen-1. *J Biol Chem* **272:** 1156–1163

Nakamura K, Manabe T, Watanabe M, Mamiya T, Ichikawa R, Kiyama Y, Sanbo M, Yagi T, Inoue Y, Nabeshima T, Mori H, Mishina M (2001) Enhancement of hippocampal LTP, reference memory and sensorimotor gating in mutant mice lacking a telencephalon-specific cell adhesion molecule. *Eur J Neurosci* **13:** 179–189

Naslavsky N, Weigert R, Donaldson JG (2004) Characterization of a nonclathrin endocytic pathway: membrane cargo and lipid requirements. *Mol Biol Cell* **15:** 3542–3552

Neumann-Giesen C, Falkenbach B, Beicht P, Claasen S, Luers G, Stuermer CAO, Herzog V, Tikkanen R (2004) Membrane and raft association of reggie-1/flotillin-2: role of myristoylation, palmitoylation and oligomerization and induction of filopodia by overexpression. *Biochem J* **378:** 509–518

Nicolaï LJ, Ramaekers A, Raemaekers T, Drozdzecki A, Mauss AS, Yan J, Landgraf M, Annaert W, Hassan BA (2010) Genetically encoded dendritic marker sheds light on neuronal connectivity in Drosophila. *Proc Natl Acad Sci USA* **107:** 20553–20558

Nijhara R, van Hennik PB, Gignac ML, Kruhlak MJ, Hordijk PL, Delon J, Shaw S (2004) Rac1 mediates collapse of microvilli on chemokine-activated T lymphocytes. *J Immunol* **173:** 4985–4993

Penzes P, Beeser A, Chernoff J, Schiller MR, Eipper BA, Mains RE, Huganir RL (2003) Rapid induction of dendritic spine morphogenesis by trans-synaptic ephrinB-EphB receptor activation of the Rho-GEF kalirin. *Neuron* **37:** 263–274

Pimplikar SW, Nixon RA, Robakis NK, Shen J, Tsai LH (2010) Amyloid-independent mechanisms in Alzheimer's disease pathogenesis. *J Neurosci* **30:** 14946–14954

Pols MS, Klumperman J (2009) Trafficking and function of the tetraspanin CD63. *Exp Cell Res* **315:** 1584–1592

Ridley AJ, Paterson HF, Johnston CL, Diekmann D, Hall A (1992) The small GTP-binding protein rac regulates growth factor-induced membrane ruffling. *Cell* **70:** 401–410

Sakagami H (2008) The EFA6 family: guanine nucleotide exchange factors for ADP ribosylation factor 6 at neuronal synapses. *Tohoku J Exp Med* **214:** 191–198

Sakagami H, Honma T, Sukegawa J, Owada Y, Yanagisawa T, Kondo H (2007) Somatodendritic localization of EFA6A, a guanine nucleotide exchange factor for ADP-ribosylation factor 6, and its possible interaction with alpha-actinin in dendritic spines. *Eur J Neurosci* **25:** 618–628

Sannerud R, Declerck I, Peric A, Raemaekers T, Menendez G, Zhou L, Veerle B, Coen K, Munck S, De Strooper B, Schiavo G, Annaert W (2011) ADP ribosylation factor 6 (ARF6) controls amyloid precursor protein (APP) processing by mediating the endosomal sorting of BACE1. *Proc Natl Acad Sci USA* **108:** E559–E568

Santy LC (2002) Characterization of a fast cycling ADP-ribosylation factor 6 mutant. *J Biol Chem* **277:** 40185–40188

Segura E, Nicco C, Lombard B, Véron P, Raposo G, Batteux F, Amigorena S, Théry C (2005) ICAM-1 on exosomes from mature dendritic cells is critical for efficient naive T-cell priming. *Blood* **106:** 216–223

Stenmark H, Parton RG, Steele-Mortimer O, Lütcke A, Gruenberg J, Zerial M (1994) Inhibition of rab5 GTPase activity stimulates membrane fusion in endocytosis. *EMBO J* **13:** 1287–1296

Stuermer C (2010) The reggie/flotillin connection to growth. *Trends Cell Biol* **20:** 6–13

Suzuki S, Kiyosue K, Hazama S, Ogura A, Kashihara M, Hara T, Koshimizu H, Kojima M (2007) Brain-derived neurotrophic factor regulates cholesterol metabolism for synapse development. *J Neurosci* **27:** 6417–6427

Swanwick C, Shapiro M, Vicini S, Wenthold R (2010a) Flotillin-1 mediates neurite branching induced by synaptic adhesion-like molecule 4 in hippocampal neurons. *Mol Cell Neurosci* **45:** 213–225

Swanwick C, Shapiro M, Vicini S, Wenthold R (2010b) Flotillin-1 promotes formation of glutamatergic synapses in hippocampal neurons. *Dev Neurobiol* **70:** 875–883

Théry C, Zitvogel L, Amigorena S (2002) Exosomes: composition, biogenesis and function. *Nat Rev Immunol* **2:** 569–579

Tian L, Nyman H, Kilgannon P, Yoshihara Y, Mori K, Andersson L, Kaukinen S, Rauvala H, Gallatin W, Gahmberg C (2000) Intercellular adhesion molecule-5 induces dendritic outgrowth by homophilic adhesion. *J Cell Biol* **150:** 243–252

Tian L, Rauvala H, Gahmberg CG (2009) Neuronal regulation of immune responses in the central nervous system. *Trends Immunol* **30:** 91–99

Tian L, Stefanidakis M, Ning L, Van Lint P, Nyman-Huttunen H, Libert C, Itohara S, Mishina M, Rauvala H, Gahmberg C (2007) Activation of NMDA receptors promotes dendritic spine development through MMP-mediated ICAM-5 cleavage. *J Cell Biol* **178:** 687–700

Tian L, Yoshihara Y, Mizuno T, Mori K, Gahmberg CG (1997) The neuronal glycoprotein telencephalin is a cellular ligand for the CD11a/CD18 leukocyte integrin. *J Immunol* **158:** 928–936

Wakabayashi Y, Tsujimura A, Matsuda K, Yoshimura N, Kawata M (2008) Appearance of LFA-1 in the initial stage of synaptogenesis of developing hippocampal neurons. *Arch Histol Cytol* **71:** 23–36

Wegner CS, Wegener CS, Malerød L, Pedersen NM, Progida C, Prodiga C, Bakke O, Stenmark H, Brech A (2010) Ultrastructural characterization of giant endosomes induced by GTPase-deficient Rab5. *Histochem Cell Biol* **133:** 41–55

Yoshihara Y, De Roo M, Muller D (2009) Dendritic spine formation and stabilization. *Curr Opin Neurobiol* **19:** 146–153

Yuste R, Bonhoeffer T (2004) Genesis of dendritic spines: insights from ultrastructural and imaging studies. *Nat Rev Neurosci* **5:** 24–34